THE EFFECT OF PULSED FOCUSED ULTRASOUND ON THE NATIVE PANCREAS

MEHDI RAZAVI[1,2], **FENGYANG ZHENG**[1,3], **ARSENII TELICHKO**[1], **MUJIB ULLAH**[1], **JEREMY DAHL**[1], **AVNESH S THAKOR**[1,*]

[1]Interventional Regenerative Medicine and Imaging Laboratory, Stanford University School of Medicine, Department of Radiology, Palo Alto, California 94304, USA

[2]Biionix™ (Bionic Materials, Implants & Interfaces) Cluster, Department of Internal Medicine, College of Medicine, University of Central Florida, Orlando, Florida 32827, USA

[3]Department of Ultrasound, Zhongshan Hospital, Fudan University and Shanghai Institute of Medical Imaging, Shanghai 200032, China

Abstract

Pulsed focused ultrasound (pFUS) utilizes short cycles of sound waves to mechanically shake cells within tissues which, in turn, causes transient local increases in cytokines, growth factors and cell adhesion molecules. While the effect of pFUS has been investigated in several different organs including the kidney, muscle, and heart, its effect on the pancreas has not been investigated. In the present work, we applied pFUS to the rodent pancreas with the following parameters: 1.1MHz frequency, 5Hz pulse repetition frequency, 5% duty cycle; 10ms pulse length; 160s duration with low intensity pFUS having: 11.5W/cm^2 spatial average temporal average intensity (I_{SATA}) and 3MPa negative peak pressure (NPP); and with high intensity pFUS having: 18.5W/cm^2 I_{SATA} and 4MPa NPP; here we found that pFUS changed the expression of several cytokines while having no effect on the underlying tissue histology or health of pancreatic cells (as demonstrated by no significant change in plasma levels of amylase and lipase). Furthermore, we demonstrated that this effect on cytokine expression in the pancreas was acoustic intensity-dependent; while pFUS at low intensities turned off the expression of several cytokines, at high intensities it had the opposite effect and turned on the expression of these cytokines. The ability to non-invasively manipulate the microenvironment of the pancreas using sound waves could have profound implications for priming and modulating this organ for the application of cellular therapies in the context of both regenerative medicine (i.e. diabetes and pancreatitis) and oncology (i.e. pancreatic cancer).

Keywords

Pulsed focused ultrasound; Pancreas; Histology; Molecular expression

*Corresponding Author: Avnesh S Thakor, MD PhD, 3155 Porter Drive, Department of Radiology, Stanford University, Palo Alto, CA, 94304, asthakor@stanford.edu, Tel: 650-723-8061, Fax: 650-736-8937.

INTRODUCTION

Focused ultrasound (FUS) is a non-invasive therapeutic modality used for the treatment of solid tumors. It works by causing temperature elevations (>60°C) at focal points while sparing the overlying and surrounding normal tissues (Hsiao et al. 2016). Continuous focused ultrasound (cFUS) has therefore been utilized for thermal ablation of tumors, relying on continuous exposures to generate heat required to induce coagulative necrosis (Burks et al. 2011). In the clinical setting, cFUS is currently being used for thermal ablation of uterine fibroids, bone tumors, desmoid tumors and prostate cancer (Golan et al. 2017). In clinical trials, cFUS is also being investigated in the setting of the pancreas for the treatment of pancreatic cancer (Li et al. 2012).

While the main mechanism of cFUS is thermal ablation, which is achieved by converting ultrasound energy to heat, there are other additional mechanical effects of cFUS including acoustic cavitation, radiation force, and acoustic streaming. Furthermore, these effects have recently attracted much attention in the application of drug delivery, gene therapy and thrombolysis (Frenkel 2008; Phenix et al. 2014; Suo et al. 2015). However, to minimize any temperature elevations and hence allow the mechanical effects of sound waves to predominate, FUS can be applied non-continuously or pulsed (i.e. pulsed focused ultrasound; pFUS); this lowers the rate of energy deposition and thus allows cooling to occur between pulses (Tempany et al. 2011). pFUS exposures, despite utilizing relatively high intensities (1000–2000 Watts/cm^2) minimize temperature elevations in tissue (no more than 4–5 °C) (Frenkel et al. 2007)(Patel et al. 2008).

Hence, studies are now showing that pFUS can be used to increase cellular and vascular permeability, and control drug release from ultrasound responsive carriers without heat deposition to the target tissues (Tempany et al. 2011). Furthermore, recent studies have investigated the molecular mechanisms and effects of pFUS in the rodent muscle (Burks et al. 2011), kidney (Ziadloo et al. 2012) and heart (Jang et al. 2017) and have shown that it increases the activation/expression of several cytokines, growth factors and cell adhesion molecules in tissues (Burks et al. 2013; Burks et al. 2015; Jang et al. 2017). However, what still remains unknown are the effects of pFUS on the pancreas.

The pancreas is a glandular organ made from two distinct components: the exocrine pancreas which is a reservoir of digestive enzymes, and the endocrine islets which can secrete metabolic related hormones including insulin (Zhou and Melton 2018). Distinct diseases can affect either the exocrine or endocrine pancreas; for instance, pancreatitis and pancreatic cancer predominantly affect the exocrine gland while diseases like diabetes affect the endocrine component of the gland (i.e. the islets). Hence, the present study will investigate the effects of pFUS on the mouse pancreas given that it could be used as non-invasive technology to modulate the pancreatic microenvironment to facilitate the effects of intrinsic or extrinsic cellular therapies in the context of both regenerative medicine (i.e. diabetes and pancreatitis) and oncology (i.e. pancreatic cancer).

MATERIALS AND METHODS

pFUS on the pancreas

i. Set-up: A therapeutic pFUS transducer (H-102NRE, Sonic Concepts, Bothell, Washington, USA) with central frequency of 1.1MHz, focal length of 55mm, aperture diameter of 64mm and central opening of 49mm was used. This transducer was driven by a function generator (Agilent 33250A, Santa Clara, California, USA) which was connected to a 50dB linear power amplifier (ENI 525LA, Rochester, New York, USA) and an impedance matching circuit (Sonic Concepts, Bothell, Washington, USA). The transducer was then calibrated in a water tank filled with degassed water. To excite the transducer during calibration, a "burst" mode consisting of 1.1MHz frequency with 20 cycles at 100Hz pulse repetition frequency (PRF) was used. A hydrophone (HNR-0500, Onda, Sunnyvale, California, USA) was placed in the focal spot of the transducer and an Acoustic Intensity Measurement System (AIMS III, Onda, Sunnyvale, California, USA) was used for precise movement and positioning of the hydrophone as well as obtaining digitized waveforms from the oscilloscope (Agilent DSO6012a, Santa Clara, California, USA). To guide pFUS, the therapeutic transducer was fitted in a custom coupling cone filled with degassed water (Figure 1a–b). The coupling cone (Sonic Concepts, Bothell, Washington, USA) was made of light transparent plastic to provide acoustic coupling between the pFUS transducer and pancreas. The cone dimensions were matched with the size and form of the H102-NRE transducer. In all experiments, the coupling cone was filled with degassed deionized water. The measured beam profile (full width half-maximum area for pressure) at focal area was 10mm long and 1.5mm in diameter. The intensity and pressure measurements were performed for negative peak pressures (NPP) up to 3MPa in order to reduce risks of hydrophone damage. The obtained intensities and NPP values were then scaled to the desired PRF and duty cycle (DC) and extrapolated to higher pressures/intensities. A typical waveform and 2D pressure map are shown in Figure 1c–d. The temperature rise during pFUS was estimated by measuring the thermal index (TI) in degassed and deionized water using a hydrophone.

ii. Treatment: Female CD1 mice (7–9 weeks of age, 28–36g) were used in all of our studies. Animals were housed under conventional conditions having access to food and water *ad libitum*. The care for all mice within the study was in accordance with the guidelines approved by the Institutional Animal Care and Use Committee (IACUC) at Stanford University. During the procedure, mice were anesthetized with isoflurane (2.5% in O_2) and placed in the supine position. Hair on the body of mice was then removed with depilatory cream and the skin was disinfected. A transversal incision was made on the left upper abdomen to expose the stomach and spleen which were covered with sterile PBS-wetted gauze immediately after exposure. The tip of the transducer was then placed above the pancreas and coupled to the organ with ultrasound gel (Aquasonic, Bio-Medical Instruments, Clinton Charter Township, Michigan, USA). Eight evenly distributed foci throughout the pancreas were treated with pFUS. The duration of each sonication was 20s with a duration of less than 5s between each sonication. The distance between spots was kept at 1mm in both the X and Y direction. The following ultrasound parameters were used: 1.1MHz frequency, 5Hz pulse repetition frequency, 5% duty cycle; 10ms pulse length; 160s

duration with low intensity pFUS having: 11.5W/cm^2 spatial average temporal average intensity (I$_{SATA}$) and 3MPa negative peak pressure (NPP); and with high intensity pFUS having: 18.5W/cm^2 I$_{SATA}$ and 4MPa NPP. For control animals, the pancreas was exposed and coupled to the transducer with ultrasound gel in the same way, but these animals received sham pFUS with no power delivered to the transducer. The selection of our pFUS parameters was based on previous literature showing these parameters were safe and effective on the mouse muscle (Burks et al. 2011), mouse kidney (Ziadloo et al. 2012), and rat heart (Jang et al. 2017). Following pFUS treatment, the skin incision was sutured and animals were left to recover.

Mice were randomly allocated into a total of 6 experimental groups (n=6 per group) consisting of 3 groups (Group 1: Sham/Control; Group 2: Low intensity pFUS and Group 3: High intensity pFUS) at 2 time points (4h and 24h). At each time point, mice were euthanized by CO$_2$ inhalation and the pancreas harvested for histological and molecular analyses.

Histological analysis of pFUS treated pancreases

Following harvesting of the pancreas, a section of the treated gland was fixed in 10% (vol./vol) neutral buffered formalin (NBF), embedded in paraffin, sectioned (5μm thick) using a HM 355S automatic microtome (ThermoFisher Scientific, Waltham, Massachusetts, USA) and stained with hematoxylin and eosin (H&E). Immunohistochemistry was also undertaken on pancreatic tissue sections using primary antibodies (AbCam) including guinea pig polyclonal antibodies to insulin (1:50) and mouse monoclonal antibodies to glucagon (1:50). All stained sections were then scanned using a NanoZoomer (Hamamatsu Photonics, Hamamatsu, Japan). To detect apoptotic cells, TUNEL staining was also performed using a fluorescein-based in situ cell death detection kit (Roche Applied Science, Penzberg, Germany) according to manufacturer's protocol.

Molecular analysis of pFUS treated pancreases

Following harvesting of the pancreas, a section of the treated pancreas was frozen using liquid nitrogen and homogenized using a tissue protein extraction reagent (ThermoFisher Scientific, Waltham, Massachusetts, USA) containing a protease inhibitor cocktail (Sigma-Aldrich, St. Louis, Missouri, USA) and Phenylmethanesulfonyl fluoride PMSF (Sigma-Aldrich, St. Louis, Missouri, USA). Homogenized tissues were then centrifuged at 15,000rpm for 20min at 4°C and the supernatants collected. To determine the total protein content, the supernatants were analyzed using bicinchoninic acid assay (ThermoFisher Scientific, Waltham, Massachusetts, USA). The supernatants with a total protein content of 3 mg/mL were then analyzed by multiplex ELISAs. For multiplex ELISAs, mouse 39 plex kits (ThermoFisher Scientific, Waltham, Massachusetts, USA) were used according to manufacturer's protocol.

Serum markers of pancreatic damage following pFUS

At the time of euthanasia, blood samples were collected from all groups of animals, centrifuged and the supernatants collected. Serum levels of amylase and lipase were then measured as indicators of pancreatic enzyme activity using the AMY Flex® reagent

cartridge, and LIPL Flex® reagent cartridge (Sigma-Aldrich, St. Louis, Missouri, USA), respectively. Animals which did not undergo any operation were used as the control group for time 0h.

Statistical analysis

All experiments were performed with 4–6 animals and the results are expressed as mean ±standard error of the mean. Statistical analysis of all quantitative data was performed using a one or two-way ANOVA (Analysis of Variance) with post-hoc Tukey tests (Prism GraphPad Software, San Diego, California, USA or Astatsa.com; Online Web Statistical Calculators, Mountain View, California, USA) with any differences considered statistically significant when P<0.05.

RESULTS

Histological analysis of pFUS treated pancreases

No significant changes were seen following histological analysis of either the exocrine or endocrine (i.e. islets) components of the pancreas following pFUS treatment. In mice that received low and high acoustic intensities of pFUS, the morphological integrity of pancreatic islets was highly preserved-Following pFUS, islets showed expression of insulin and glucagon similar to control animals. Using a TUNEL assay, there was also no evidence of any increased apoptosis in pancreatic tissue samples following pFUS treatment at both low and high acoustic intensities (Figure 2).

Molecular analysis of pFUS treated pancreases

i.   Low intensity pFUS: Compared to control animals, pancreases treated with low intensity pFUS did not show any changes in cytokines expression at 4h (P>0.05). However, at 24h pancreases showed a significant down-regulation in expression of: granulocyte colony-stimulating factor (GCSF: −57±1%), granulocyte-macrophage colony-stimulating factor (GMCSF: −60±2%), interferon-alfa (IFN-α: −46±1%), Interferon-gamma (IFN-γ: −76±1%), interleukin-10 (IL-10:−67±1%), IL-12P70 (−42±4%), IL-13 (−62±2%), IL-15 (−70±1%), IL-17α (−75±1%), IL-18 (−56±2%), IL-1α (−70±2%), IL-1β (−70±4%), IL-2 (−67±3%), IL-23 (−73±3%), IL-27 (−51±1%), IL-28 (−78±6%), IL-3 (−79±1%), IL-31 (−71±2%), IL-4 (−61±2%), IL-5 (−73±1%), IL-6 (−42±5%), IL-9 (−55±2%), interferon gamma-induced protein 10 (IP-10: −81±13%), LEPTIN (−45±1%), leukemia inhibitory factor (LIF: −56±1%), lipopolysaccharide-induced CXC chemokine (LIX: −56±1%), macrophage colony-stimulating factor (MCSF: −67±3%), MCP-3 (−43±8%), macrophage inflammatory protein 1 alfa (MIP-1α: −72±3%), MIP-1β (−78±9%), MIP-2 (−62±2%), transforming growth factor beta 1 (TGF-β: −44±7%), tumor necrosis factor alpha (TNF-α: −73±2%), and vascular endothelial growth factor (VEGF: −23±1%) (Figure 3, P<0.05).

ii.   High intensity pFUS: When the intensity of pFUS was increased from low to high, this led to a significant increase in expression of EOTAXIN, GCSF, GMCSF, IFN-γ, IL-15, IL-6, and MCP-3 at 4h following pFUS treatment when compared to control animals. After 24h, the expression of multiple cytokines in treated pancreases significantly increased when compared to control animals: GCSF (+33±2%), GMCSF (+36±2%), growth-regulated

oncogene-alfa (GRO-α; +55±5), IFN-γ (44±5%),1L-12P70 (45±4%), IL-13 (67±5%), IL-15 (38±1%), IL-17α (24±2%), IL-18 (49±3%), IL-1α (43±5%), IL-1β (64±5%), IL-2 (44±5%), IL-23 (28±3%), IL-28 (92±10%), IL-3 (61±4%), IL-31 (76±4%), IL-4 (41±2%), IL-5 (26±1%), IL-6 (49±7%), IL-9 (60±5%), LEPTIN (42±1%), LIF (+25±1), LIX (64±3%), MIP-2 (57±4%), regulated on activation, normal T cell expressed and secreted (RANTES: 80±14%), TGF-β (53±2%), and TNF-α (47±2%) (Figure 3, P<0.05).

Serum markers of pancreatic damage following pFUS

i. Amylase: The serum amylase level in mice who had their pancreas treated with high pFUS was 2526±210 U/L at 4h following treatment, however, this significantly decreased to 1029±72 U/L at 24h. Control mice (i.e. mice which received a sham procedure-surgery alone with no pFUS) had an amylase level of 1697±155 U/L at 4h which significantly decreased to 975±55 U/L at 24h (P<0.05). Compared to normal animals (i.e. mice which did not receive any sham surgery or pFUS), both pFUS treated and control animals had a slightly higher serum amylase level at 4h (2526±210 and 1697±155 vs. 1045±115 U/L). Although this difference was statistically significant (P<0.05), this was not the case by 24h as both pFUS treated and control animals had returned to normal levels (Figure 4a; 1029±72 U/L and 975±55 U/L vs. 1045±115 U/L; P>0.05).

ii. Lipase: The serum lipase level in mice who had their pancreas treated with high pFUS was 447±113 U/L at 4h following treatment, however, this significantly decreased to 103±8 U/L at 24h. Control mice (i.e. mice which received a sham procedure-surgery alone with no pFUS) had an amylase level of 263±79 U/L at 4h which significantly decreased to 122±11 U/L at 24h (P<0.05). No significant difference was found between the lipase level of mice which treated with pFUS and control mice at both time points (P>0.05). Compared to normal animals (i.e. mice which did not receive any sham surgery or pFUS), both pFUS treated and control animals had a slightly higher serum amylase level at 4h (447±113 and 263±79 vs. 108±10 U/L). Although this difference was statistically significant (P<0.05), this was not the case by 24h as both pFUS treated and control animals had returned to normal levels (Figure 4b; 103±8 and 122±11 vs. 108±10 U/L; P>0.05).

DISCUSSION

In our study, we used a similar frequency and duty cycle as reported in prior studies (Burks et al. 2015)(Burks et al. 2011)(Ziadloo et al. 2012)(Jang et al. 2017), however we utilized a lower I_{SATA}. Previous studies investigating the molecular mechanisms and effects of pFUS in rodent muscle (Burks et al. 2011), kidney (Ziadloo et al. 2012) and heart (Jang et al. 2017) and have shown that pFUS increases the activation/expression of several cytokines, growth factors and cell adhesion molecules. Here, we applied pFUS to the mouse pancreas and analyzed the corresponding histological and molecular effects within this organ. The pancreas is unusually sensitive to mechanical injury and it has long been recognized that manipulation of the pancreas at the time of surgery can induce acute pancreatitis complicating postoperative recovery; hence, manipulation of the pancreas is always minimized whenever possible during surgery (Romac et al. 2018). Therefore, we selected a lower I_{SATA} (i.e. 11.5W/cm^2 for low pFUS and 18.5W/cm^2 for high pFUS) compared to the

I_{SATA} used in by Burks et al. (2011) (i.e. 133W/cm^2) to minimize the possibility of mechanical or thermal injury.

Our goal was to safely administer pFUS to the pancreas with no adverse effects. Our results show that pFUS, at the intensities used in this study, can be safely administered to the pancreas with no adverse histological effects. Interestingly, pFUS was found to modulate the microenvironment of the pancreas and these effects were dependent on the acoustic intensity of pFUS; at low intensities, there was down-regulation in the expression of several cytokines/molecular markers, while at high intensities this effect was reversed with upregulation in the expression of several cytokines/molecular markers.

FUS is a noninvasive treatment modality that can be coupled with imaging guidance (e.g. ultrasound or magnetic resonance imaging) to accurately focus sound waves with a relatively small focal zone (typically 1mm × 1mm × 10mm) to structures deep within the body without causing effects on the intervening tissues (Clement 2004; Jiang et al. 2009; N'Djin et al. 2011). While cFUS causes thermal ablation of tissue, pFUS uses shorter pulsed exposures (10– 50ms/s) to provide lower energy deposition and allowing cooling to occur between pulse intervals thereby minimizing temperature elevations in tissue (Frenkel et al. 2007; Patel et al. 2008). Instead, this allows the non-thermal effects of FUS (i.e. acoustic cavitation and acoustic radiation forces) to predominate. An estimate of the temperature increase, based on the TI measured in water using the hydrophone setup, was 1.2 and 2.1 for low and high dose pFUS, respectively.

Previous characterizations of the cellular and molecular responses to pFUS have not shown significant long term deleterious effects. For example, although pFUS exposure to the brain was shown to produce indiscrete lesions (McDannold et al. 2005; Sheikov et al. 2008), and even though there was limited extravasation of red blood cells and infiltration of macrophages which persisted up to 4 weeks, these effects did not appear to induce neuronal damage, necrosis, or apoptosis (McDannold et al. 2005). pFUS exposures to the muscle also suggest that pFUS, unlike FUS, can be applied to tissues without causing cellular destruction (Burks et al. 2011). Currently, clinical trials are ongoing to investigate the application of cFUS in the treatment of pancreatic cancer; initial results show that cFUS is safe and can be applied non-invasively to the pancreas despite its sensitive nature, deep location and intricate relationship to major blood vessels. This is important as minor trauma to the pancreas can result in the release of pancreatic enzymes which can cause life-threatening pancreatitis (Sung et al. 2011). In keeping with this, we also confirmed that pFUS, at both low and high acoustic intensities, had no detrimental effect on the pancreas as determined histologically (i.e. preservation of the morphology of both the exocrine and endocrine components of the pancreas), using TUNEL assays (i.e. to measure markers of cellular apoptosis within the pancreas) and following analysis of the serum (i.e. levels of amylase and lipase which are key indicators that are used to diagnose pancreatitis (Lin et al. 2006)). For the later variable, the levels of both amylase and lipase were raised at 4h but then decreased by 24h. However, this effect is not likely attributed to pFUS given that even control animals experienced this trend; instead, this is likely due to the effect of having to minimally invasively expose the pancreas in order to apply pFUS to the gland. While this effect was seen in our study, it would not be seen in humans given that pFUS can target the pancreas non-invasively.

Unfortunately, this was not possible in our study given that the native pancreas in small animal models, such as the mouse, cannot be easily visualized and identified in vivo using either ultrasound or magnetic resonance imaging.

Following the application of pFUS to the pancreas, we observed molecular changes in the pancreas as demonstrated by alterations in the expression of various cytokines, growth factors and cell adhesion molecules. Previous studies have also demonstrated that pFUS is able to modulate the microenvironment of other tissues/organs including muscle (Burks et al. 2011), kidney (Burks et al. 2015) and heart (Jang et al. 2017). Indeed, pFUS has been shown to trigger acute and short-lived cascade of cytokines and growth factors which are involved in macrophage infiltration, wound healing, and anti-inflammatory responses (Burks et al. 2011). However, what is interesting is that we observed a differential effect on the molecular profile of the pancreas depending on whether low or high acoustic intensities of pFUS were employed. In general, our results showed that when pFUS was applied at low acoustic intensities it down regulated cytokine expression in the pancreas and at high intensities it up regulated cytokine expression. However, the differential effect we have observed can possibly be explained by either direct effects of sound waves on the cells of the pancreas (i.e. their ability to exert mechanical effects which then get translated into molecular changes via a process of mechanotransduction (Burks et al. 2011)) or indirect effects of sound waves on the neuronal supply to cells (i.e. the ability to modulate the activity of autonomic or peripheral neurons via a process of neuromodulation (Kubanek 2018; Sato et al. 2018)).

At low acoustic intensities, pFUS induced a down-regulation in the expression of both angiogenic growth factors (i.e. MCSF, VEGF, and TGF-β) as well as several key pro-inflammatory cytokines (i.e. IP-10, IL-6, IL-1β, TNF-α, IFN-γ, and IL-2) at 24h post-pFUS. In the setting of the pancreas, MCSF, VEGF, and TGF-β have been shown to induce proliferation of hematopoietic and cancer cells while also promoting angiogenesis (Eubank et al. 2003; Holmes and Zachary 2005; Viñals and Pouysségur 2001); hence down-regulation of these factors could have a key role in modulating the tumor microenvironment and hence pancreatic tumor growth. In the setting of diabetes, IP-10, IFN-γ, and IL-2 have been shown to participate in the autoimmune response that leads to destruction of β-cells within the pancreatic islets; hence down-regulation of these cytokines following pFUS at low acoustic intensities could have a role in slowing the progression of diabetes. Finally, IL-6, IL-1β, and TNF-α have been shown to play a key role in in acute pancreatitis (AP) and pancreatic tumor progression (Lewis et al. 2006; Viedma et al. 1992; Zhao et al. 2016) so their downregulation could be important in attenuating the progression of both of these diseases.

At high acoustic intensities, pFUS induced an up-regulation in the expression of angiogenic growth factors (i.e. TGF-β, and MCP-1) as well as pro-inflammatory cytokines (i.e. TNF-α, IFN-γ, and IL-1β), at 24h post-pFUS. This effect could be very important in the setting of tissue regeneration where TGF-β has been shown to accelerate vascularization (Krafts 2010) and MCP-1 can provide an important signal for mesenchymal stem cell (MSC) homing (Belema-Bedada et al. 2008; Nitzsche et al. 2017). In the latter scenario, pFUS could be applied to enable spatio-temporal control over the homing of unmodified MSCs (Burks et al. 2015). In support of this, Burks et al (Burks et al. 2011)(Burks et al. 2013) and Ziadloo et al

(Ziadloo et al. 2012) previously characterized homing of i.v. MSCs after pFUS to healthy skeletal muscle and kidney. Similar to our study, they found that pFUS can create a transient molecular zip-code consisting of localized changes in the level of different cytokines (Burks et al. 2013). The evidence therefore suggests pFUS can elicit local molecular responses through mechanotransduction, which can promote the homing of circulating MSCs. For instance, given that our study has shown that pro-inflammatory cytokines (i.e. TNF-α, IFN-γ, and IL-1β) are also up-regulated following high pFUS, this may prove advantageous for creating an environment which can facilitate the homing of MSCs to the pancreas for organ regeneration. Another consideration would be that pFUS-induced changes to the organ microenvironment can alter MSCs function after homing occurs. Several studies have found that treating MSCs with various factors in vitro (prior to infusion) enhances their therapeutic capabilities in vivo. For example, pretreating MSCs with IFN-γ resulted in both increased production of IL-10 and reduced levels of TNF-α in a mouse model of inflammatory bowel disease (Duijvestein et al. 2011). Another study pretreated MSCs with IFN-γ and then either TNF-α, IL-1α, or IL-1β and found all three combinations improved outcomes in mouse models of graft-versus-host disease and delayed-type hypersensitivity (Kavanagh et al. 2014). Interestingly, studies have also shown that the cocktail of TNF-α, IL-1β, and IFN-γ can direct the differentiation of pancreatic ductal cells towards the endocrine lineage (Valdez et al. 2016) and hence this may be important in the setting of regenerating the pancreas following its destruction in the setting of either diabetes or pancreatitis. Hence, pFUS could either precondition the target organ to both enhance MSC homing and/or stimulate different cell signaling pathways (Burks et al. 2015)(Burks et al. 2015)(Burks et al. 2015).

In summary, pFUS is able to induce changes in the molecular microenvironment of the pancreas without adversely affecting the pancreatic gland. These changes are dependent on the acoustic intensity and future studies will be undertaken to fully evaluate the mechanisms responsible for these changes as well as the implications of these changes in different disease states.

Supplementary Material

Refer to Web version on PubMed Central for supplementary material.

ACKNOWLEDGEMENT

REFERENCES

Belema-Bedada F, Uchida S, Martire A, Kostin S, Braun T. Efficient Homing of Multipotent Adult Mesenchymal Stem Cells Depends on FROUNT-Mediated Clustering of CCR2. Cell Stem Cell 2008;2:566–575. [PubMed: 18522849]

Burks SR, Nguyen BA, Tebebi PA, Kim SJ, Bresler MN, Ziadloo A, Street JM, Yuen PST, Star RA, Frank JA. Pulsed focused ultrasound pretreatment improves mesenchymal stromal cell efficacy in preventing and rescuing established acute kidney injury in mice. Stem Cells 2015;33:1241–1253. [PubMed: 25640064]

Burks SR, Ziadloo A, Hancock HA, Chaudhry A, Dean DD, Lewis BK, Frenkel V, Frank JA. Investigation of cellular and molecular responses to pulsed focused ultrasound in a mouse model. PLoS One 2011;6.

Burks SR, Ziadloo A, Kim SJ, Nguyen BA, Frank JA. Noninvasive pulsed focused ultrasound allows spatiotemporal control of targeted homing for multiple stem cell types in murine skeletal muscle and the magnitude of cell homing can be increased through repeated applications. Stem Cells 2013;31:2551–2560. [PubMed: 23922277]

Clement GT. Perspectives in clinical uses of high-intensity focused ultrasound. Ultrasonics 2004;42:1087–1093. [PubMed: 15234170]

Duijvestein M, Wildenberg ME, Welling MM, Hennink S, Molendijk I, Van Zuylen VL, Bosse T, Vos ACW, De Jonge-Muller ESM, Roelofs H, Van Der Weerd L, Verspaget HW, Fibbe WE, Te Velde AA, Van Den Brink GR, Hommes DW. Pretreatment with interferon-γ enhances the therapeutic activity of mesenchymal stromal cells in animal models of colitis. Stem Cells 2011;29:1549–1558. [PubMed: 21898680]

Eubank TD, Galloway M, Montague CM, Waldman WJ, Marsh CB. M-CSF Induces Vascular Endothelial Growth Factor Production and Angiogenic Activity From Human Monocytes. J Immunol 2003;171:2637–2643. Available from: http://www.jimmunol.org/cgi/doi/10.4049/jimmunol.171.5.2637 [PubMed: 12928417]

Frenkel V. Ultrasound mediated delivery of drugs and genes to solid tumors. Adv. Drug Deliv. Rev 2008 pp. 1193–1208. [PubMed: 18474406]

Frenkel V, Oberoi J, Stone MJ, Park M, Deng C, Wood BJ, Neeman Z, Horne M, Li KCP. Pulsed High-Intensity Focused Ultrasound Enhances Thrombolysis in an in Vitro Model. Radiology 2007;239:86–93.

Golan R, Bernstein AN, McClure TD, Sedrakyan A, Patel NA, Parekh DJ, Marks LS, Hu JC. Partial Gland Treatment of Prostate Cancer Using High-Intensity Focused Ultrasound in the Primary and Salvage Settings: A Systematic Review. J. Urol 2017 pp. 1000–1009. [PubMed: 28433640]

Holmes DIR, Zachary I. The vascular endothelial growth factor (VEGF) family: Angiogenic factors in health and disease. Genome Biol. 2005.

Hsiao YH, Kuo SJ, Der Tsai H, Chou MC, Yeh GP. Clinical application of high-intensity focused ultrasound in cancer therapy. J. Cancer 2016 pp. 225–231. [PubMed: 26918034]

Jang KW, Tu TW, Nagle ME, Lewis BK, Burks SR, Frank JA. Molecular and histological effects of MR-guided pulsed focused ultrasound to the rat heart. J Transl Med 2017;15. [PubMed: 28100276]

Jiang Z, Holyoak GR, Bartels KE, Ritchey JW, Xu G, Bunting CF, Slobodov G, Piao D. In vivo trans-rectal ultrasound–coupled optical tomography of a transmissible venereal tumor model in the canine pelvic canal. J Biomed Opt 2009;14:030506. [PubMed: 19566288]

Kavanagh DPJ, Robinson J, Kalia N. Mesenchymal Stem Cell Priming: Fine-tuning Adhesion and Function. Stem Cell Rev Reports 2014;10:587–599.

Krafts KP. Tissue repair: The hidden drama. Organogenesis. 2010 pp. 225–233. [PubMed: 21220961]

Kubanek J. Neuromodulation with transcranial focused ultrasound. Neurosurg Focus 2018;44:E14.

Lewis AM, Varghese S, Xu H, Alexander HR. Interleukin-1 and cancer progression: The emerging role of interleukin-1 receptor antagonist as a novel therapeutic agent in cancer treatment. J. Transl. Med 2006.

Li PZ, Zhu SH, He W, Zhu LY, Liu SP, Liu Y, Wang GH, Ye F. High-intensity focused ultrasound treatment for patients with unresectable pancreatic cancer. Hepatobiliary Pancreat Dis Int 2012;11:655–660. [PubMed: 23232639]

Lin X-Z, Wang S-S, Tsai Y-T, Lee S-D, Shiesh S-C, Pan H-B, Su C-H, Lin C-Y. Serum Amylase, Isoamylase, and Lipase in the Acute Abdomen. J Clin Gastroenterol 2006;11:47–52.

McDannold N, Vykhodtseva N, Raymond S, Jolesz FA, Hynynen K. MRI-guided targeted blood-brain barrier disruption with focused ultrasound: Histological findings in rabbits. Ultrasound Med Biol 2005;31:1527–1537. [PubMed: 16286030]

N'Djin WA, Melodelima D, Schenone F, Rivoire M, Chapelon JY. Assisted hepatic resection using a toroidal HIFU device: An in vivo comparative study in pig. Med Phys 2011;38:1769–1778. [PubMed: 21626911]

Nitzsche F, Müller C, Lukomska B, Jolkkonen J, Deten A, Boltze J. Concise Review: MSC Adhesion Cascade—Insights into Homing and Transendothelial Migration. Stem Cells. 2017 pp. 1446–1460. [PubMed: 28316123]

Patel PR, Luk A, Durrani A, Dromi S, Cuesta J, Angstadt M, Dreher MR, Wood BJ, Frenkel V. In vitro and in vivo evaluations of increased effective beam width for heat deposition using a split focus high intensity ultrasound (HIFU) transducer. Int J Hyperth 2008;24:537–549.

Phenix CP, Togtema M, Pichardo S, Zehbe I, Curiel L. High intensity focused ultrasound technology, its scope and applications in therapy and drug delivery. J. Pharm. Pharm. Sci 2014 pp. 136–153.

Romac JMJ, Shahid RA, Swain SM, Vigna SR, Liddle RA. Piezo1 is a mechanically activated ion channel and mediates pressure induced pancreatitis. Nat Commun 2018;9. [PubMed: 29339724]

Sato T, Shapiro MG, Tsao DY. Ultrasonic Neuromodulation Causes Widespread Cortical Activation via an Indirect Auditory Mechanism. Neuron 2018;98:1031–1041.e5. [PubMed: 29804920]

Sheikov N, McDannold N, Sharma S, Hynynen K. Effect of Focused Ultrasound Applied With an Ultrasound Contrast Agent on the Tight Junctional Integrity of the Brain Microvascular Endothelium. Ultrasound Med Biol 2008;34:1093–1104. [PubMed: 18378064]

Sung HY, Jung SE, Cho SH, Zhou K, Han JY, Han ST, Kim J Il, Kim JK, Choi JY, Yoon SK, Yang JM, Han CW, Lee YS. Long-term outcome of high-intensity focused ultrasound in advanced pancreatic cancer. Pancreas 2011;40:1080–1086. [PubMed: 21926543]

Suo D, Guo S, Lin W, Jiang X, Jing Y. Thrombolysis using multi-frequency high intensity focused ultrasound at MHz range: An in vitro study. Phys Med Biol 2015;60:7403–7418. [PubMed: 26350754]

Tempany CMC, McDannold NJ, Hynynen K, Jolesz FA. Focused Ultrasound Surgery in Oncology: Overview and Principles. Radiology 2011;259:39–56. [PubMed: 21436096]

Valdez IA, Dirice E, Gupta MK, Shirakawa J, Teo AKK, Kulkarni RN. Proinflammatory Cytokines Induce Endocrine Differentiation in Pancreatic Ductal Cells via STAT3-Dependent NGN3 Activation. Cell Rep 2016;15:460–470. [PubMed: 27068459]

Viedma JA, Pérez-Mateo M, Domínguez JE, Carballo F. Role of interleukin-6 in acute pancreatitis comparison with C-reactive protein and phospholipase A. Gut 1992;33:1264–1267. [PubMed: 1427382]

Viñals F, Pouysségur J. Transforming growth factor beta1 (TGF-beta1) promotes endothelial cell survival during in vitro angiogenesis via an autocrine mechanism implicating TGF-alpha signaling. Mol Cell Biol 2001;21:7218–30. Available from: http://www.ncbi.nlm.nih.gov/pubmed/11585905%0Ahttp://www.pubmedcentral.nih.gov/articlerender.fcgi?artid=PMC99897 [PubMed: 11585905]

Zhao X, Fan W, Xu Z, Chen H, He Y, Yang G, Yang G, Hu H, Tang S, Wang P, Zhang Z, Xu P, Yu M. Inhibiting tumor necrosis factor-alpha diminishes desmoplasia and inflammation to overcome chemoresistance in pancreatic ductal adenocarcinoma. Oncotarget 2016;7:81110–81122. [PubMed: 27835602]

Zhou Q, Melton DA. Pancreas regeneration. Nature. 2018 pp. 351–358.

Ziadloo A, Burks SR, Gold EM, Lewis BK, Chaudhry A, Merino MJ, Frenkel V, Frank JA. Enhanced homing permeability and retention of bone marrow stromal cells by noninvasive pulsed focused ultrasound. Stem Cells 2012;30:1216–1227. [PubMed: 22593018]
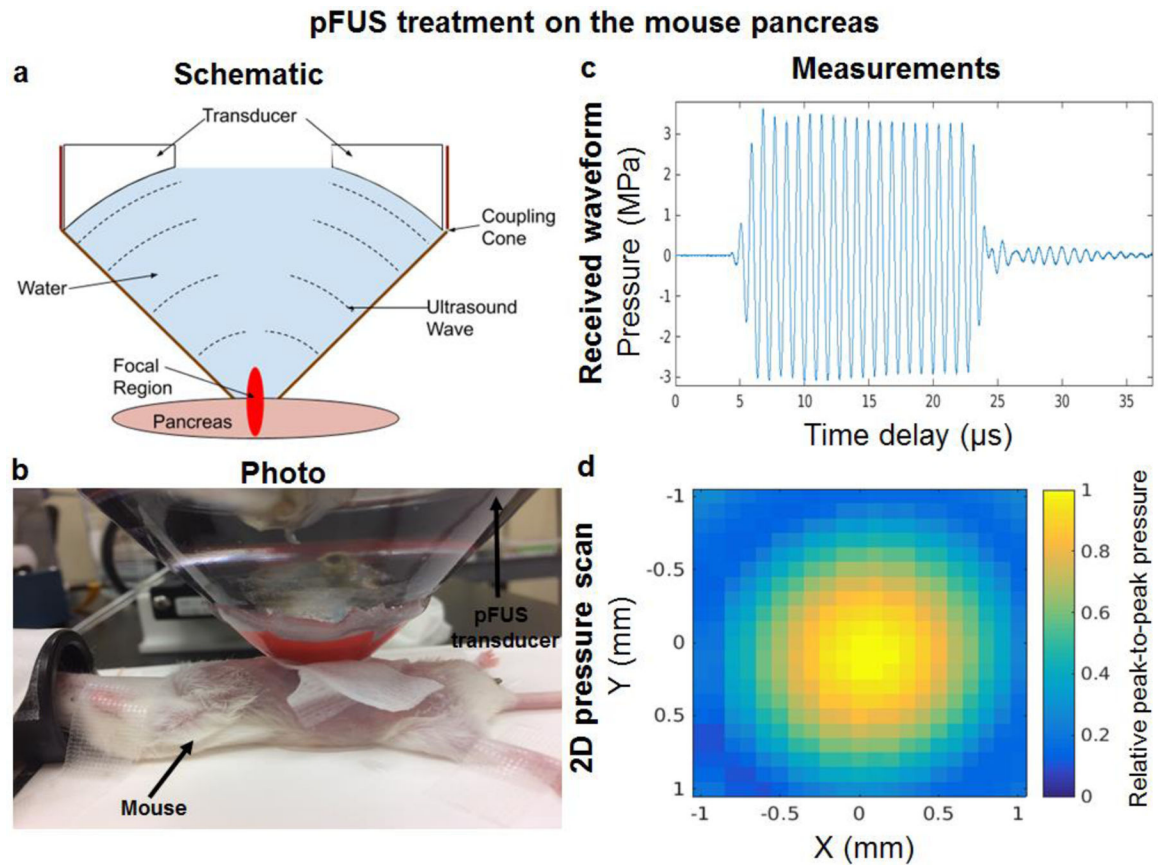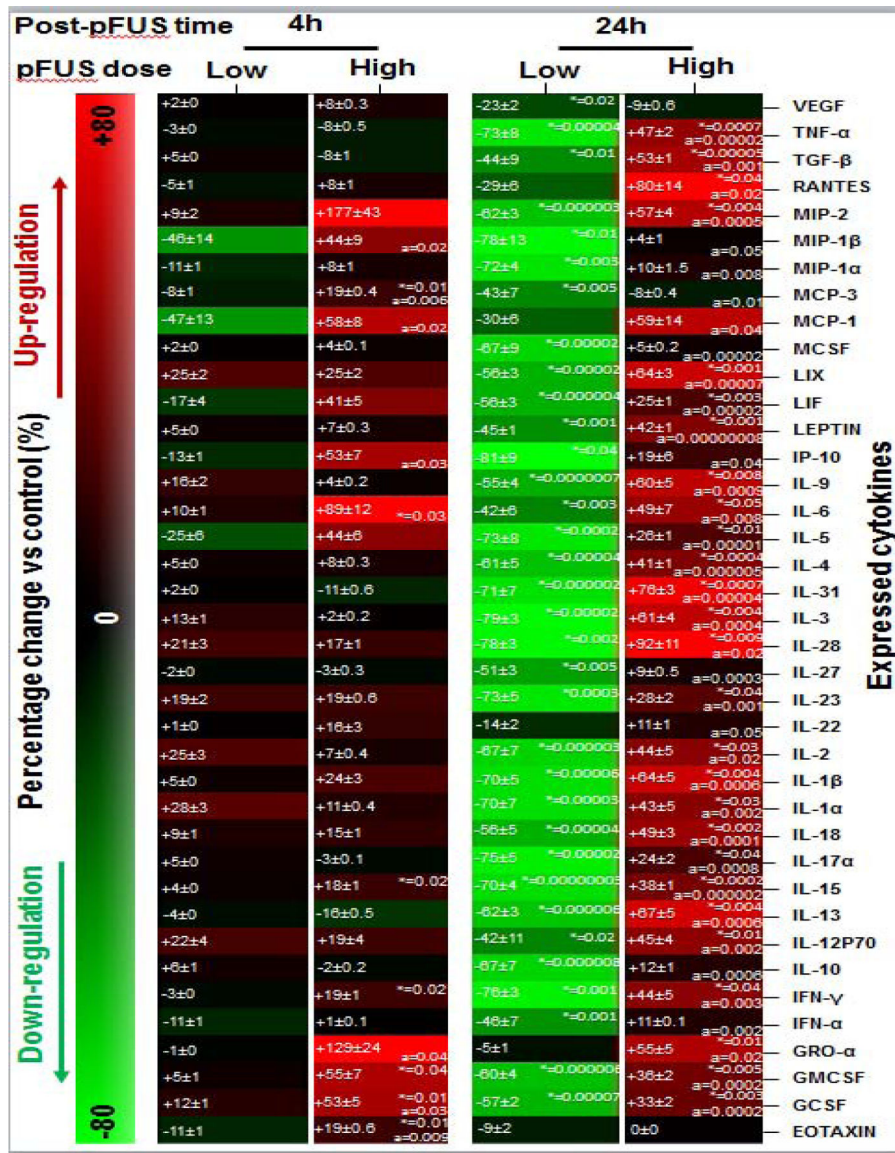
Figure 1. pFUS treatment on the pancreas:
(a-b) pFUS guidance to the mouse pancreas using a therapeutic transducer fitted in a custom cone and filled with degassed water ((a) side-view and (b) top-view). The transmitted ultrasound waves are produced by a function generator, amplified through the amplifier at a constant gain and emitted from the transducer face to eight evenly distributed foci throughout the mouse pancreas; **(c)** The typical waveform and **(d)** 2D pressure map measured (full width half-maximum area for pressure) at a focal area (10mm long × 1.5mm diameter).
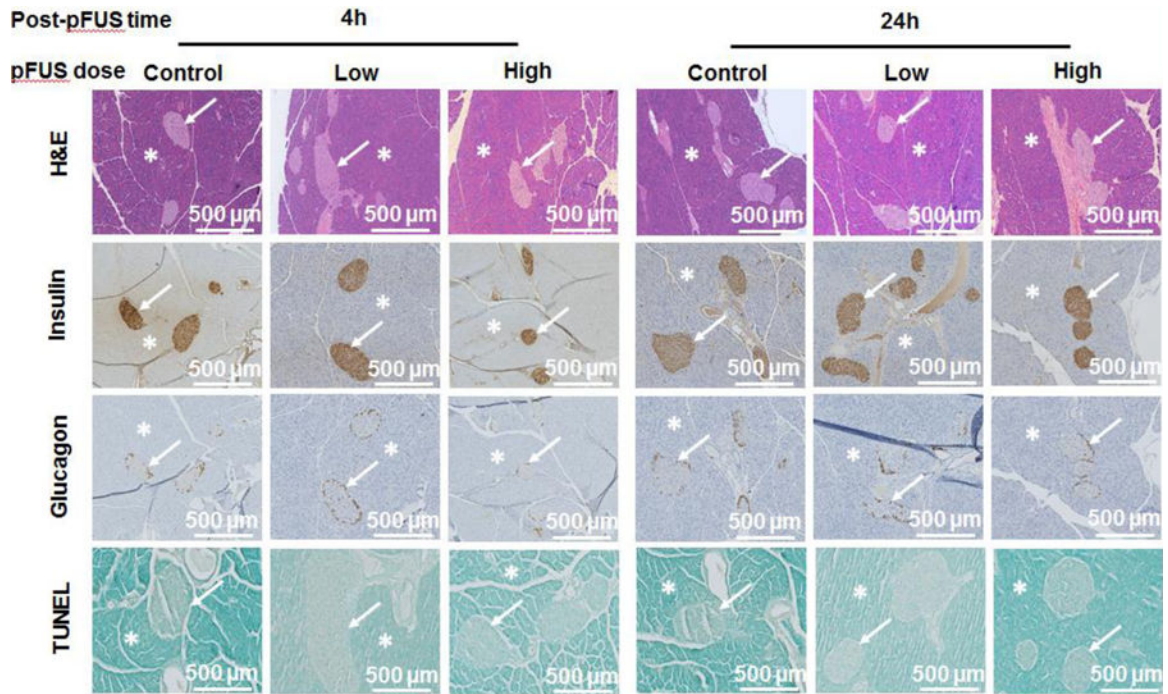
Figure 2. Histological analysis of pFUS treated pancreases:
Samples of pFUS treated pancreases stained with H&E, insulin, glucagon and TUNEL.

Asterisks show exocrine and arrows show endocrine (i.e. islets) components of the pancreas.

Figure 3. Molecular analysis of pFUS treated pancreases:
Molecular expression profile of the pancreas following pFUS treatment relative to control mice. In each box, the left side values are mean±SEM and right side are P-values. Significant differences: *P<0.05: pFUS treated pancreas vs. control, [a]P<0.05: high dose vs. low dose (Two-way ANOVA post-hoc Tukey Test).
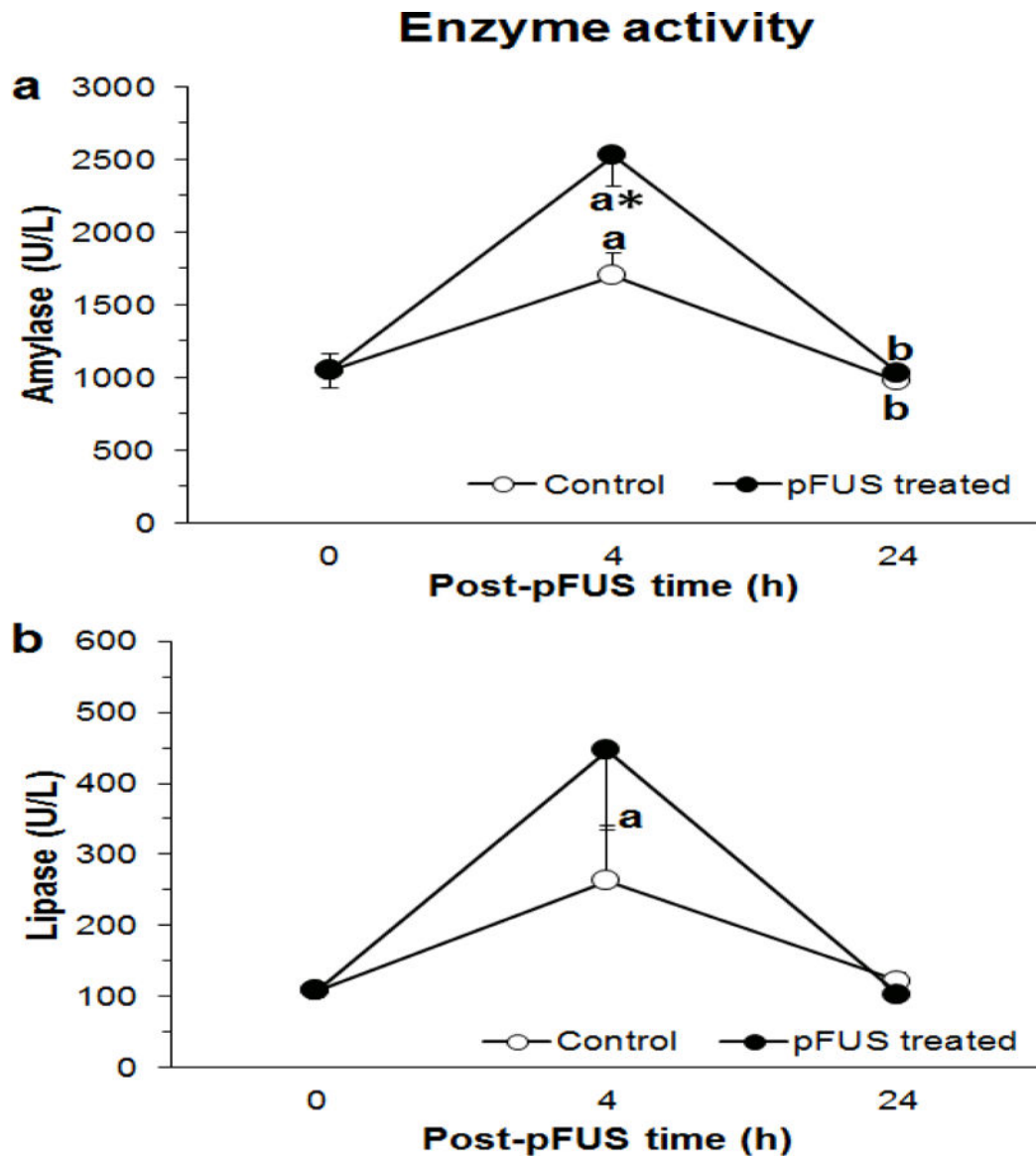
Enzyme activity

Figure 4. Serum markers of pancreatic damage following pFUS:
Serum levels of (a) amylase and (b) lipase as indicators of pancreatic enzyme activity measured from normal mice (i.e. time point 0h) and mice whose pancreases were treated with pFUS and control mice which received a sham surgical procedure.
Significant differences: [a]P<0.05: 4h vs. 0h and 24h vs. 0h, [b]P<0.05: 24h vs. 4h, and *P<0.05: pFUS treated pancreas vs. control (unpaired t-test).